Atmos. Chem. Phys., 18, 12683–12698, 2018
https://doi.org/10.5194/acp-18-12683-2018

Atmospheric Chemistry and Physics
Open Access
EGU

Radiative feedbacks of dust in snow over eastern Asia in CAM4-BAM

Xiaoning Xie[1], Xiaodong Liu[1,2], Huizheng Che[3], Xiaoxun Xie[1], Xinzhou Li[1], Zhengguo Shi[1], Hongli Wang[4], Tianliang Zhao[5], and Yangang Liu[6]

[1]SKLLQG, Institute of Earth Environment, Chinese Academy of Sciences, Xi'an 710061, China
[2]University of Chinese Academy of Sciences, Beijing 100049, China
[3]Key Laboratory for Atmospheric Chemistry, Institute of Atmospheric Composition,
Chinese Academy of Meteorological Sciences, CMA, Beijing 100081, China
[4]Shaanxi Radio and TV University, Xi'an 710119, China
[5]Key Laboratory for Aerosol-Cloud-Precipitation of China Meteorological Administration,
Nanjing University of Science Information & Technology, Nanjing 210044, China
[6]Environmental and Climate Sciences Department, Brookhaven National Laboratory, Upton, NY 11973-5000, USA

Correspondence: Xiaoning Xie (xnxie@ieecas.cn)

Received: 10 April 2018 – Discussion started: 7 May 2018
Revised: 13 August 2018 – Accepted: 16 August 2018 – Published: 31 August 2018

Abstract. Dust in snow on the Tibetan Plateau (TP) could reduce the visible snow albedo by changing surface optical properties and removing the snow cover through increased snowmelt, which leads to a significant positive radiative forcing and remarkably alters the regional energy balance and the eastern Asian climate system. This study extends our previous investigation in dust–radiation interactions to investigate the dust-in-snow radiative forcing (SRF) and its feedbacks on the regional climate and the dust cycle over eastern Asia through the use of the Community Atmosphere Model version 4 with a Bulk Aerosol Model parameterizations of the dust size distribution (CAM4-BAM). Our results show that SRF increases the eastern Asian dust emissions significantly by 13.7 % in the spring, countering a 7.6 % decrease in the regional emissions by the dust direct radiative forcing (DRF). SRF also remarkably affects the whole dust cycle, including transport and deposition of dust aerosols over eastern Asia. The simulations indicate an increase in dust emissions of 5.1 %, due to the combined effect of DRF and SRF. Further analysis reveals that these results are mainly due to the regional climatic feedbacks induced by SRF over eastern Asia. By reducing the snow albedo over the TP, the dust in snow mainly warms the TP and influences its thermal effects by increasing the surface sensible and latent heat flux, which in turn increases the aridity and westerly winds over northwestern China and affects the regional dust cycle. Additionally, the dust in snow also accelerates the snow-melting process, reduces the snow cover and then expands the eastern Asian dust source region, which results in increasing the regional dust emissions. Hence, a significant feature of SRF on the TP is the creation of a positive feedback loop that affects the dust cycle over eastern Asia.

1 Introduction

A large amount of desert dust from eastern Asian arid and semiarid regions is emitted into the atmosphere, which can be carried over the wide downwind regions, including eastern China and the Pacific Ocean, and also deposited in snow over the Tibetan Plateau (Wake et al., 1994; Zhang et al., 1997; Zhao et al., 2006). The dust can significantly affect the global and regional energy balance, climate and hydrological cycle by dust direct radiative forcing and dust-in-snow radiative forcing (Ramanathan et al., 2001; Shao et al., 2011; Mahowald et al., 2014; Huang et al., 2014; Qian et al., 2015).

Dust in the atmosphere can directly absorb and scatter the thermal (longwave) and solar (shortwave) radiation, known as dust direct radiative forcing (DRF). Note that the importance of DRF in general circulation models (GCMs) has been

recognized for many years (Tegen and Lacis, 1996; Miller and Tegen, 1998; Yue et al., 2009; Mahowald et al., 2014). On the global scale, the dust DRF is about $-0.4\,\mathrm{W\,m^{-2}}$, with a range between -0.30 and $-0.6\,\mathrm{W\,m^{-2}}$, estimated by the current models described by Huneeus et al. (2011) and reviewed by Kok et al. (2017). The DRF with particle size distribution for dust from Kok (2011) is less cooling (smaller forcing effect) because atmospheric dust is coarser than represented in current models. The new size distribution results in a DRF range between -0.48 and $+0.2\,\mathrm{W\,m^{-2}}$, including the possibility that dust causes a net warming of the planet (Kok et al., 2017). The regional DRF over Asia is significantly higher than that at the global scale due to the larger dust loading, influencing the regional climate (Lau et al., 2006; Zhang et al., 2009; Han et al., 2012; Sun et al., 2012; Guo and Yin, 2015; Gu et al., 2016). A so-called elevated heat pump effect due to atmospheric heating by elevated absorbing aerosols strengthens large-scale atmospheric circulation and increases the precipitation in the late boreal spring and early summer season over the foothills of the Himalayas and northern India (Lau et al., 2006). The aerosol heating reduces the Tibetan and Himalayan snowpack cover by 6–10 %, exacerbating the greenhouse warming effect (Lau et al., 2010). The net surface and top-of-atmosphere radiative fluxes are decreased by DRF, cause a surface cooling over eastern Asia and increase the regional local stability (Zhang et al., 2009). Dust loading in spring and summer influences the eastern Asian summer monsoon through affecting atmospheric circulation and thermal structures induced by DRF (Sun et al., 2012; Guo and Yin, 2015). Gu et al. (2016) claimed that the circulation and precipitation responses to DRF are different over southeastern Asia and northern Africa, which is dependent on the location of dust relative to the rainfall ranges.

Depositions of light-absorbing aerosols on snow (e.g., black carbon – BC – and dust) can reduce the visible snow albedo by changing surface optical properties and remove snow cover by increasing snowmelt in entirely or partially snow-covered areas, resulting in significant positive radiative forcing (Hansen and Nazarenko, 2004; Xu et al., 2009; Huang et al., 2011; Qian et al., 2015). Based on previous studies (Hansen and Nazarenko, 2004; Hansen et al., 2005), IPCC (2007) showed the radiative forcing range of $0.10 \pm 0.10\,\mathrm{W\,m^{-2}}$ induced by aerosol in snow at the global scale, whereas IPCC (2013) adopted a radiative forcing of $+0.04$ ($+0.02$ to $+0.09$) $\mathrm{W\,m^{-2}}$ according to the results of Bond et al. (2013). Recent studies have shown the significant impacts of snow grain shape (spherical vs. nonspherical) and aerosol–snow mixing state (internal vs. external) on BC and dust-in-snow radiative forcing (e.g., Flanner et al., 2012; Liou et al., 2014; Dang et al., 2016; He et al., 2017b, 2018a). Further studies also show the effects of snow grain packing (He et al., 2017a) and aerosol size distribution in snow (Schwarz et al., 2013; He et al., 2018b) on aerosol–snow interactions. The Tibetan Plateau (TP) is a vast, elevated

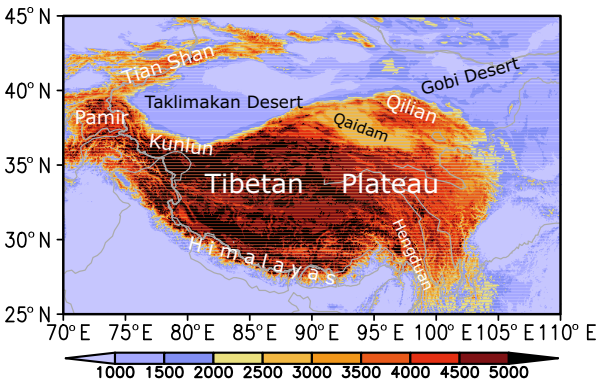

Figure 1. Terrain of the Tibetan Plateau (unit: m) including major mountains (Kunlun, Himalayas, Hengduan, Qilian and Tian Shan), Pamir Plateau, Qaidam Basin deserts and its surrounding deserts (Taklimakan and Gobi deserts).

plateau with an average elevation of 4500 m located in Asia (Fig. 1). In addition to being close to the Taklimakan (one of the largest sand deserts in the world) and Gobi deserts, the TP also has several deserts (e.g., Qaidam Basin desert) within it and is near the industrial regions in the Indian subcontinent and eastern China. There exists a larger amount of deposition on snow of black carbon and dust aerosols over the TP due to the high industrial and natural emissions in Asia from observational studies (Xu et al., 2009; Ming et al., 2013; Qu et al., 2014; Lee et al., 2017; Li et al., 2018; Zhang et al., 2018). Over this region, the particles of dust are the dominant insoluble impurities compared with black carbon in terms of particle mass (Ming et al., 2013; Qu et al., 2014). These studies further claim that the impacts of dust aerosols on snow albedo and dust-induced surface radiative forcing exceed those of black carbon over the TP, mainly because of larger dust loading. The aerosol-induced snow albedo perturbation generates much larger positive surface radiative flux changes of 5–25 $\mathrm{W\,m^{-2}}$ during spring over the TP (Flanner et al., 2009; Qian et al., 2011). Furthermore, Qian et al. (2011) claimed that absorbing aerosol in snow can cause a 1.0 °C warming over the TP, which can influence the eastern Asian and southern Asian monsoon through the TP's thermal and dynamical forcing.

Dust cycles, including dust emissions, transport, and dry and wet depositions, are altered by DRF through affecting the atmospheric vertical thermal structures and surface wind speed. The mechanism of PBL (the planetary boundary layer) (Miller et al., 2004; Perez et al., 2006; Heinold et al., 2007) was initially proposed to explain the reduction of dust emissions induced by DRF (Perlwitz et al., 2001). It was described that the surface negative net DRF reduces the turbulent flux of surface sensible heat and reduces PBL mixing. A positive feedback between DRF and dust emissions is shown through the PBL mechanism over northern Africa due to the surface positive net DRF. An alternative mechanism was pro-

posed that DRF produces an anomaly in the surface pressure, especially on the edge of the dust layer, resulting in impacts on circulation and wind speed (Ahn et al.,2007; Heinold et al., 2008).

In our previous study (Xie et al., 2018), we showed, using the improved Community Atmosphere Model version 4 with a Bulk Aerosol Model parameterization of the dust size distribution (CAM4-BAM), that DRF decreases the eastern Asian dust cycle owing to the negative surface radiative forcing through the PBL mechanism, which counteracts northern African dust emissions induced by DRF. Considering that the dust cycle change by the dust-in-snow radiative forcing (SRF) over eastern Asia has not been studied previously. Using the identical CAM4-BAM model, we extend the DRF effects (Xie et al., 2018) to systematically to investigate the SRF, the regional climate change and the dust cycle change induced by the SRF over eastern Asia. In addition, we compare CAM4-BAM with the DRF effects discussed in Xie et al. (2018). The rest of this paper is structured as follows. In Sect. 2, we first review the improved CAM4-BAM model based on Albani et al. (2014) and Xie et al. (2018) and describe the experimental design. The model performance is also evaluated against the temporal and spatial observations of snow cover and surface temperature. The model results for dust radiative forcing and its radiative feedbacks are discussed with regard to the region of study in Sect. 3. Further discussions and conclusions are summarized in Sects. 4 and 5, respectively.

2 Model evaluation and experimental design

2.1 CAM4-BAM and experiments

The CAM4 model described in detail by Neale et al. (2010) is the atmospheric component of the Community Climate System Model version 4 (CCSM4). The CAM4-BAM model considers a sub-bin fixed size distribution of externally mixed sulfate, sea salt, organic carbon, black carbon, and dust by Tie et al. (2005). The improvements to CAM4-BAM for the dust cycle were proposed based on three major aspects: the optimized soil erodibility maps with respect to each of the macroareas, updated optical properties of dust with realistic absorption parameters and a new size distribution for dust emissions, which better represents the dust cycle, most notably the improved size distribution (Albani et al., 2014). The new size distribution decreases the emitted fraction of clay aerosols ($< 2\,\mu m$) in excellent agreement with measurements and exerts a smaller cooling compared to the released version. This improved model can be used to investigate the eastern Asian dust cycle and the DRF over this region (Xie et al., 2018). Black carbon and mineral dust in snow were represented in the Snow, Ice, and Aerosol Radiative (SNICAR) component (Flanner et al., 2007, 2009), which has been used to investigate the aerosol-in-snow forcing at the global scale (Flanner et al., 2009) and at the regional scale (Qian et al., 2011). Note that a set of new parameters including the effects of snow grain shape and aerosol–snow mixing state have been included in the SNICAR model, which may represent the realistic snowpack situation (He et al., 2018c). It will be interesting to observe the difference in radiative forcing between these two models in the future.

Table 1. Description of the model experiments in this work. Here DRF represents dust direct radiative forcing and SRF is defined as dust-in-snow radiative forcing.

Experiments	Simulated time	DRF	SRF
Case1	21 years (1-year spin-up)	Yes	Yes
Case2	21 years (1-year spin-up)	Yes	No
Case3	21 years (1-year spin-up)	No	No

In this work, the improved CAM4-BAM model adopts the finite volume (FV) scheme for the dynamical core with a higher horizontal resolution ($0.9^\circ \times 1.25^\circ$) and with 26 levels in the vertical direction. All the model simulations were run for the year 2000 and constrained with the sea surface temperature (SST), sea-ice concentrations and atmospheric forcings including solar irradiance, the tropospheric and stratospheric ozone, and greenhouse gases during this period. The SST and sea-ice concentration were from a merged version of the HadISST (Rayner et al., 2003) and the optimum interpolation SST data sets described by Hurrell et al. (2008). We conducted three numerical experiments including a 21-year free run with a 1-year spin-up (no nudging), one with both DRF and SRF (Case1), one with the DRF and without the SRF (Case2), and the other one without the DRF and the SRF (Case3), as summarized in Table 1. Here, it is noted that we only consider the dust aerosols in these three numerical experiments and neglect the radiative properties of other aerosols including sulfate, sea salt, organic carbon and black carbon in the improved CAM4-BAM model. Based on these three experiments, i.e., Case1, Case2 and Case3, we can derive the DRF (Case2 − Case3), the SRF (Case1 − Case2) and the total radiative forcing (DRF+SRF, Case1 − Case3). Hence, we use the results of the differences between these three experiments to investigate the climatic feedback of SRF and the dust cycle changes induced by SRF over eastern Asia; we also compared these with changes induced solely by DRF. Due to the complex topography of the TP, higher-resolution simulations can resolve more details of the deep valleys and high mountains over and around the TP and make some significant improvements in the simulated climate (Li et al., 2015). Therefore, it is necessary to conduct the higher-resolution simulations to address this issue.

2.2 Model evaluation

This subsection assesses the climatological features, including the simulated dust aerosol optical depth (AOD) at

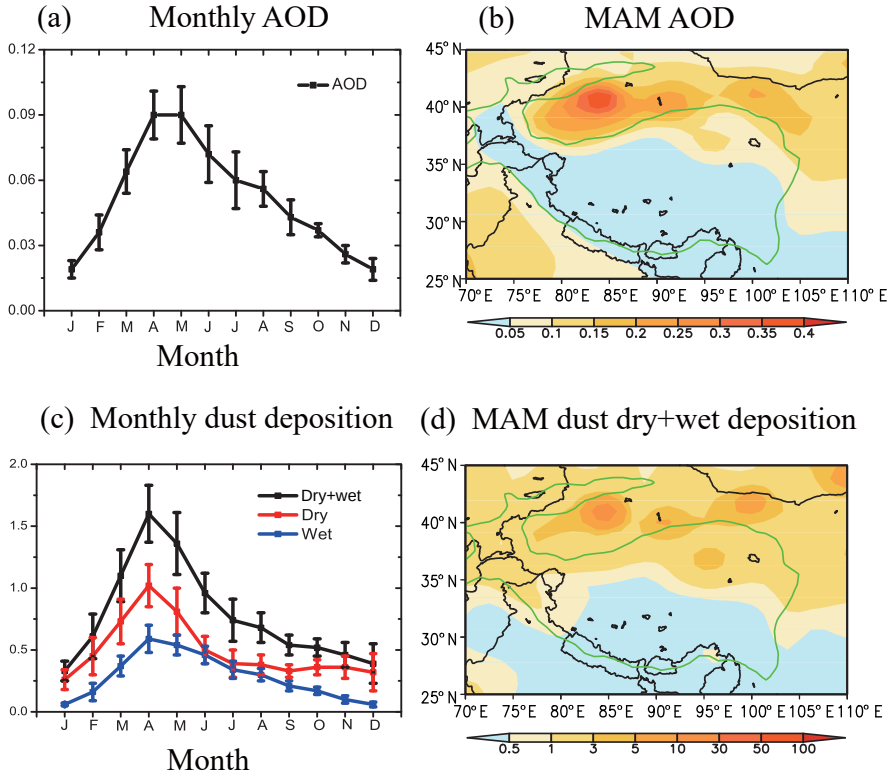

Figure 2. **(a)** Monthly dust AOD and **(b)** spatial distribution of the March–April–May (MAM) averaged AOD from the CAM4-BAM model over the Tibetan Plateau (70–110° E and 25–45° N). **(c)** Monthly dust deposition ($\mu g\,m^{-2}\,s^{-1}$) including dust dry, wet and dry+wet deposition and **(d)** spatial distribution of the MAM averaged total dust deposition (dry+wet, $\mu g\,m^{-2}\,s^{-1}$) over this region. Note that the error bars **(a, c)** represent the standard deviation of the corresponding variables, and the green outlined area **(b, d)** indicates the plateau above 2500 m.

550 nm, dust deposition, snow cover and surface temperature in order to evaluate the impacts of dust-in-snow forcing over the TP. Figure 2a shows the monthly dust AOD over the TP from the CAM4-BAM model. It shows that the dust AOD has the largest values (> 0.06) in MAM (March–April–May), likely because of the higher frequency of dust storms over this region in MAM. Figure 2b displays the spatial distribution of the simulated MAM dust AOD from CAM4-BAM. This simulated spatial distribution shows that the dust AOD has larger values over dust source regions (Gobi and Taklimakan deserts), where dust AOD values are greater than 0.2, particularly over the Taklimakan desert. Figure 2c shows the monthly mean dust deposition over the TP, including dry, wet and total (dry+wet) depositions, indicating the largest dust deposition in MAM. This phenomenon of the monthly variation of dust deposition is very similar to the dust AOD (Fig. 2a). It is noted that the dry deposition of dust is much larger than the wet deposition probably because of less rain over northwestern China and its seasonal precipitation (Lau et al., 2006; Xu et al., 2008; Kang et al., 2010). Figure 2d shows that the total dust deposition exhibits two peaks over the two dust source regions. Additionally, deserts in the western and northeastern regions of TP exhibit peaks in dust deposition, which we expect will further increase the SRF signal. This improved CAM4-BAM has been evaluated against measurements such as AOD and dust deposition over the eastern Asia (Albani et al., 2014; Xie et al., 2018), showing a better simulation of the dust cycle.

Figure 3 shows the monthly mean snow cover fraction (SCF) and surface temperature over the TP from the model and observations (MODIS SCF and CRU (Climatic Research Unit) surface temperature data). The MODIS data show a larger SCF in the winter and spring over the TP, with the maximum reaching approximately 25 % in January (Fig. 3a). The corresponding minimum SCF occurs in July and August. Overall, the CAM4-BAM model can capture the monthly variations of SRF, with the minimum in summer and the maximum in winter and spring. But the model overestimates the amplitude of the monthly variations of SCF, overestimates SCF in winter and spring and underestimates SCF in summer. The overestimated SCF variation is probably due to the model's coarse horizonal resolution ($0.9° \times 1.5°$) and smooth terrain (Qian et al., 2011; Lee et al., 2013). Figure 4a shows that the MAM consistently snow-covered ar-

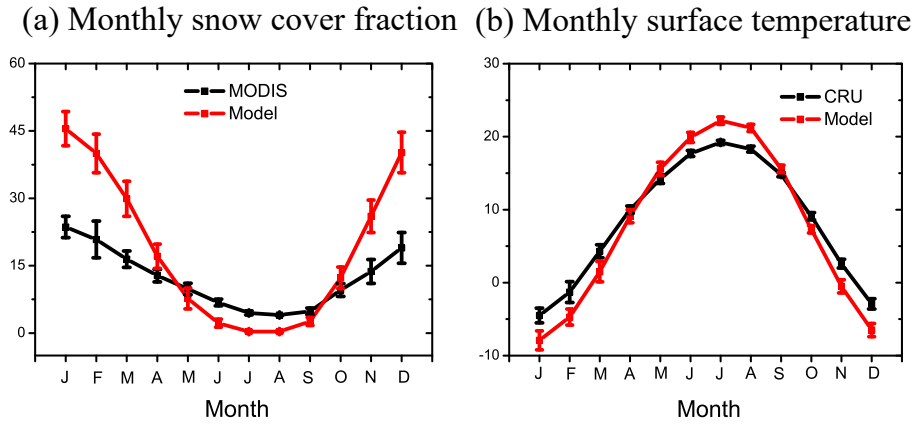

Figure 3. (a) Monthly snow cover fraction (%) from MODIS and the CAM4-BAM model; **(b)** monthly surface temperature (°C) from CRU and the CAM4-BAM model over the Tibetan Plateau (25–45° N, 70–110° E), where the error bars represent the standard deviation of the corresponding variables.

eas with SRF > 50 % are located in the western TP (including the Pamir Plateau, Tian Shan and Kunlun mountains), the southeast TP (Hengduan mountain), Himalayas, and Qilian mountains. The model can capture the most consistently snow-covered areas (Fig. 4b). In contrast to the case of SCF, the data from the Climatic Research Unit (CRU) show a lower surface temperature in winter and spring and a higher surface temperature in summer (Fig. 3b). Furthermore, the CAM4-BAM model can better capture the spatial distribution (Fig. 4c) and the monthly variations of the surface temperature (Fig. 4d), although it also overestimates the amplitude of monthly variations in the surface temperature.

3 Dust radiative forcing and its radiative feedbacks

3.1 Dust cycle changes induced by SRF

It has been documented that mineral dust can influence the atmospheric vertical thermal structures and surface wind speed by DRF, which affects the dust cycle through various mechanisms (Perlwitz et al., 2001; Miller et al., 2004; Perez et al., 2006; Heinold et al., 2007, 2008; Ahn et al., 2007; Colarco et al., 2014; Xie et al., 2018). However, the dust cycle change induced by the SRF over eastern Asia has previously not been studied systematically, despite reported large surface positive SRF over the TP (Flanner et al., 2009; Qian et al., 2011). This subsection fills this gap to examine the SRF-induced dust cycle changes during MAM over eastern Asia, including dust emissions, dust transport (defined as the vertically integrated dust flux, which is similar to water vapor transport), and the dry and wet depositions. A comparison with the DRF is also made to estimate their relative contributions.

Figure 5 shows the spatial distribution of the dust cycle changes induced by DRF (left column), SRF (middle column) and the total radiative forcing (DRF+SRF, right column) over eastern Asia in MAM; the corresponding averaged values are summarized in Table 2 over the eastern Asian dust source area (75–115° E and 25–50° N). Figure 5a shows that DRF decreases the dust emissions over this region by −7.6 %, which is −8.8 Tg per season, shown in Table 2. The corresponding dust transport and dry and wet depositions in Fig. 5d, g and j are also decreased over this region by DRF, with the magnitudes of −6.4 %, −5.7 % and −1.8 %, respectively. Figure 5b shows that SRF markedly increases the dust emissions over the eastern Asian dust source area, with 14.78 Tg per season (13.7 %), which is statistically significant. It is noted that the changes of the dust emissions induced by SRF are approximately 2 times larger than that by DRF. The changes of dust transport and dry and wet depositions (Fig. 5e, h and k) are also increased by SRF with 6.9 %, 11.9 % and 4.7 %, respectively.

Figure 5c, f, i and l show the changes in the dust cycle induced by the dust total radiative forcing. The dust emissions are significantly affected (in Fig. 5c) by the dust total radiative forcing over eastern Asia by 5.1 % with an increase of 5.98 Tg per season. It is noted that the total change in dust emissions induced by SRF+DRF is 5.98 Tg per season, which is an exact figure. However, the changes caused by DRF (−8.8 Tg per season) and SRF (14.78 Tg per season) are included in the nonlinear interactions between SRF and DRF. Hence, the values of dust emissions caused by DRF and SRF can be altered when removing the nonlinear interactions between SRF and DRF. This is because the changes in dust emissions induced by the SRF are much larger than those induced by the DRF. The dry and wet depositions are also increased (5.5 % and 2.9 %) in Fig. 5i and l by the dust total radiative forcing. Figure 5f shows the dust transport is increased over the northern part of the eastern Asian dust source region, although the averaged value of the dust transport is slightly decreased by −0.9 % (shown in Table 2) over this region due to the decreased dust transport over the southern region. In summary, the dust total radiative forcing in-

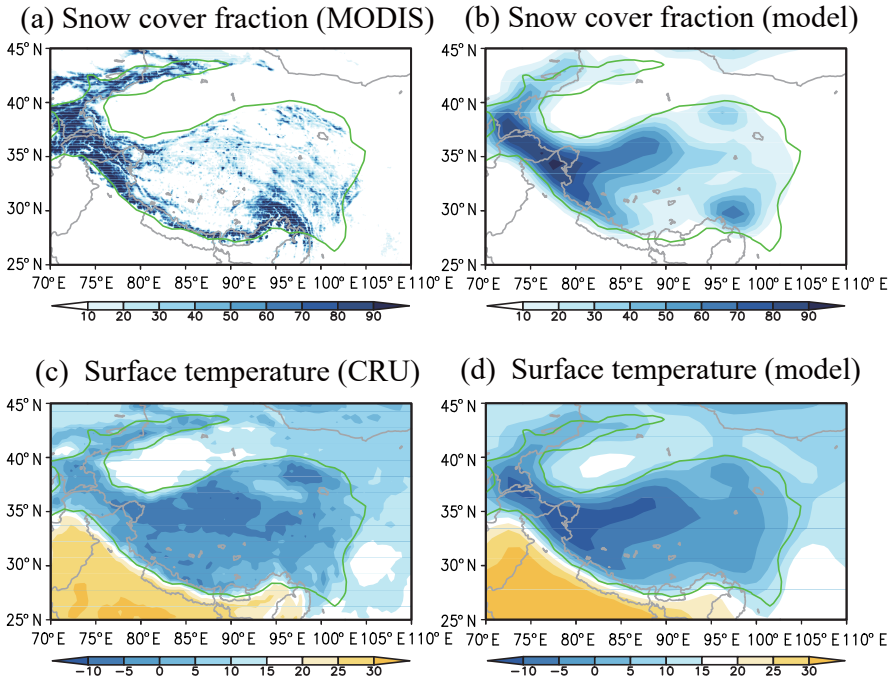

Figure 4. Spatial distribution of the MAM averaged **(a)** snow cover fraction (%) derived from MODIS for 2002–2012 and **(c)** surface temperature (°C) from CRU for 1979–2012, compared with the simulated MAM averaged **(b)** snow cover and **(d)** surface temperature for 20 model years over Tibetan Plateau. The green outlined area indicates the plateau above 2500 m.

Table 2. The March–April–May (MAM) averaged dust emissions (Tg per season), transport (g m^{-1} s^{-1}), dry deposition (Tg per season) and wet deposition (Tg per season) over the eastern Asian dust source area (75–115° E and 25–50° N) in Case1, Case2 and Case3, as well as the corresponding differences between these three experiments.

	Dust emission	Dust transport	Dry deposition	Wet deposition
Case1	122.40	1.08	68.92	36.99
Case2	107.62	1.01	61.59	35.33
Case3	116.42	1.09	65.33	35.96
DRF (Case2 − Case3)	−8.80 (−7.6 %)	−0.07 (−6.4 %)	−3.74 (−5.7 %)	−0.63 (−1.8 %)
SRF (Case1 − Case2)	14.78 (13.7 %)	0.07 (6.9 %)	7.33 (11.9 %)	1.66 (4.7 %)
DRF+SRF (Case1 − Case3)	5.98 (5.1 %)	−0.01 (−0.9 %)	3.59 (5.5 %)	1.03 (2.9 %)

creases the dust cycles, because the SRF-induced effects are much stronger than the diminishment caused by DRF.

3.2 Dust radiative forcing and the dust-induced changes in surface properties

It is noted that these dust cycle changes induced by the DRF, the SRF and the dust total radiative forcing (Fig. 5) are mainly due to the corresponding radiative forcing and its climatic feedbacks. This section examines the dust-induced radiative forcing, including DRF and SRF and its climatic feedbacks, especially with regard to the SRF.

Figure 6a shows the spatial distribution of the simulated surface albedo in MAM for Case1. Evidently, there exists a larger broadband surface albedo over the TP, especially over the western TP due to larger SCF (Fig. 4b). Compared to the MODIS surface albedo over the TP (Meng et al., 2018), the CAM4-BAM model captures its spatial distribution during MAM. However, the model overestimates the surface albedo, which is similar to multi-model ensembles' results (Li et al., 2016), mainly due to the overestimated SCF and the neglect of BC in snow. Dust in snow can decrease the snow albedo over entirely or partially snow-covered areas as mentioned above. Figure 6b shows that dust in snow significantly reduces the broadband surface albedo over the TP and its surrounding mountains, especially over the western TP (reaching over −0.1). The decrease in snow albedo mainly results from a positive feedback process: absorbing aerosols deposited on snow → reducing surface albedo → increasing surface net solar radiation → increasing surface tempera-

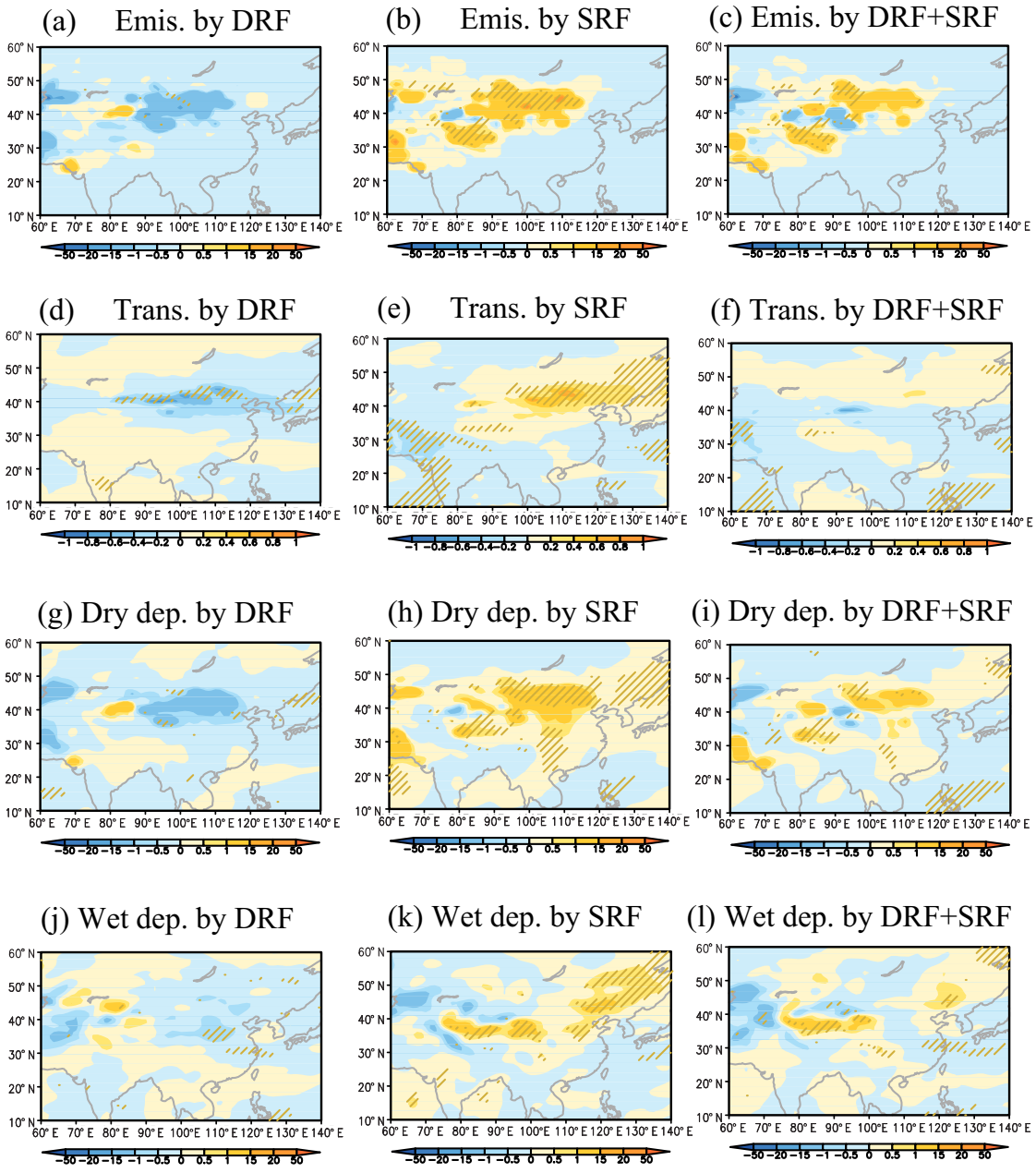

Figure 5. Dust cycle changes including **(a, b, c)** dust emissions ($g\,m^{-2}$ per season), **(d, e, f)** dust transport ($g\,m^{-1}\,s^{-1}$), **(g, h, i)** dust dry deposition ($g\,m^{-2}$ per season) and **(j, k, l)** dust wet deposition ($g\,m^{-2}$ per season) in MAM induced by dust direct radiative forcing (DRF), dust-in-snow radiative forcing (SRF) and total forcing (DRF+SRF). The slanted lines represent the grid points where the changes pass the two-tailed t test at the 5 % significance level.

ture → reducing snow fraction and depth → finally reducing surface albedo, which was proposed by Qian et al. (2011). Another element in this positive feedback process is that increasing surface temperature results in stronger snow aging and hence larger snow effective grain sizes and reduces snow albedo (Flanner et al., 2009).

Figure 7 shows the dust-induced changes in the surface radiative forcing and surface temperature in MAM by the DRF, the SRF and the total radiative forcing. The DRF displays a surface negative radiative forcing over eastern Asia, where it is much larger and statistically significant over the Taklimakan and Gobi deserts (Fig. 7a). This is mainly because the high scattering efficiency of large amounts of dust aerosols over these two dust source regions results in a larger surface negative radiative forcing. This surface negative radiative forcing reduces the surface sensible heat and then de-

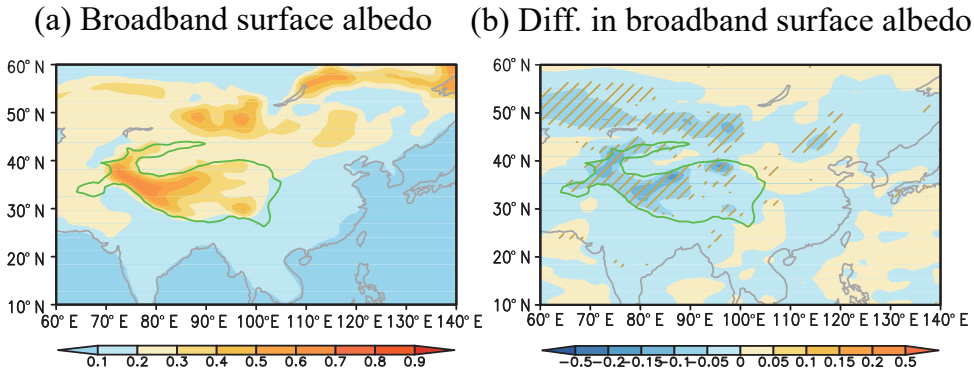

Figure 6. (a) Spatial distribution of the broadband surface albedo in MAM (Case1) and **(b)** its changes between Case1 and Case2, which are induced by dust-in-snow radiative forcing (SRF). The slanted lines represent the grid points where the changes pass the two-tailed t test at the 5 % significance level. The green outlined area indicates the plateau above 2500 m.

creases vertical mixing within the PBL and the wind speed at the surface, decreasing the regional dust emissions (labeled by the PBL mechanism) over eastern Asia (Xie et al., 2018). It is noted that this PBL mechanism was initially shown and proved by Miller et al. (2004), Perez et al. (2006) and Heinold et al. (2007). Figure 7b also shows a slightly decreased surface temperature of between −1 and 0 °C over eastern Asia, likely because of the surface negative radiative forcing.

In contrast, Fig. 7c shows that SRF displays a significant surface positive radiative forcing over the whole TP and the surrounding mountains, especially over the western TP (above 20 W m^{-2}). The decreased surface albedo over the TP (Fig. 6b) causes increasing surface net solar radiation and shows a surface positive radiative forcing over this region. This positive surface radiative forcing significantly warms the whole TP, especially the western TP (beyond 2 °C) in Fig. 7d. Figure 7e shows that the total dust radiative forcing exerts a significant and larger surface positive radiative forcing over the whole TP, compared to a significant and smaller surface negative radiative forcing over the Taklimakan and Gobi deserts. Over the TP, the SRF mainly dominates the total radiative forcing and the DRF determines the total radiative forcing over the deserts and the wide downwind regions. Hence, the surface temperature significantly increases over the TP due to the larger total positive forcing in Fig. 7f, which is determined by the SRF. Hence, we will focus on the changes in the surface properties induced by the SRF in the following sections.

Figure 8a shows the spatial distribution of the changes in the SCF induced by the SRF. The SCF is significantly decreased by the SRF over the whole TP and its surrounding mountains, where the maximum decrease of the SCF can reach above 15 %. The warming TP (Fig. 7d) due to dust in snow accelerates snow melting, reduces the snow cover and then expands the dust source region area, resulting in an increase in regional dust emissions. Figure 8b shows the significant increase in the surface latent heat flux (LHF) by the SRF. This is due to the increased soil moisture induced by a rise in the amount of snowmelt over the TP. Additionally, the increased surface precipitation during spring and summer by the SRF also increases the soil moisture, as examined in the following subsection. The warming of the TP also increases the regional surface sensible heat flux (SHF) in Fig. 8c. The total surface heat flux (LHF+SHF) shows a larger value over the TP, especially over the western TP (reaching over 10 W m^{-2}). Hence, dust in snow over the TP can warm the TP and enhance its thermal effects by increasing the surface LHF and SHF, thereby affecting the Asian climate. It is noted that SRF significantly increases the surface temperature, reduces the SCF and affects the surface total heat flux (LHF and SHF) over the TP, which is identical to the previous results (Qian et al., 2011). Due to the higher horizontal resolution of $\sim 1°$ in this study, our results show the finer spatial distribution of changes in these properties, especially over the TP compared to Qian et al. (2011).

3.3 Dust-induced climatic feedbacks

It is known that the TP, sometimes referred to as the Third Pole, can influence the Indian and eastern Asian summer monsoon and inland precipitation through its dynamical and thermal effects (e.g., Boos and Kuang, 2010; Wu et al., 2012; Liu and Dong, 2013; Shi et al., 2014; Sha et al., 2015). Qian et al. (2011) claimed that the absorbing aerosols (especially the black carbon) in snow over the TP change the eastern and southern Asian monsoon climate and hydrological cycle by the increased TP thermal effects. Here, we concentrate on the increased TP thermal effects due to dust in snow on the climate over the arid and semiarid regions of northwestern China.

Figure 9 shows the changes in the zonal wind component and the omega (vertical velocity, Pa s^{-1}) in a vertical cross section at 75–115° E in MAM, induced by the SRF. It

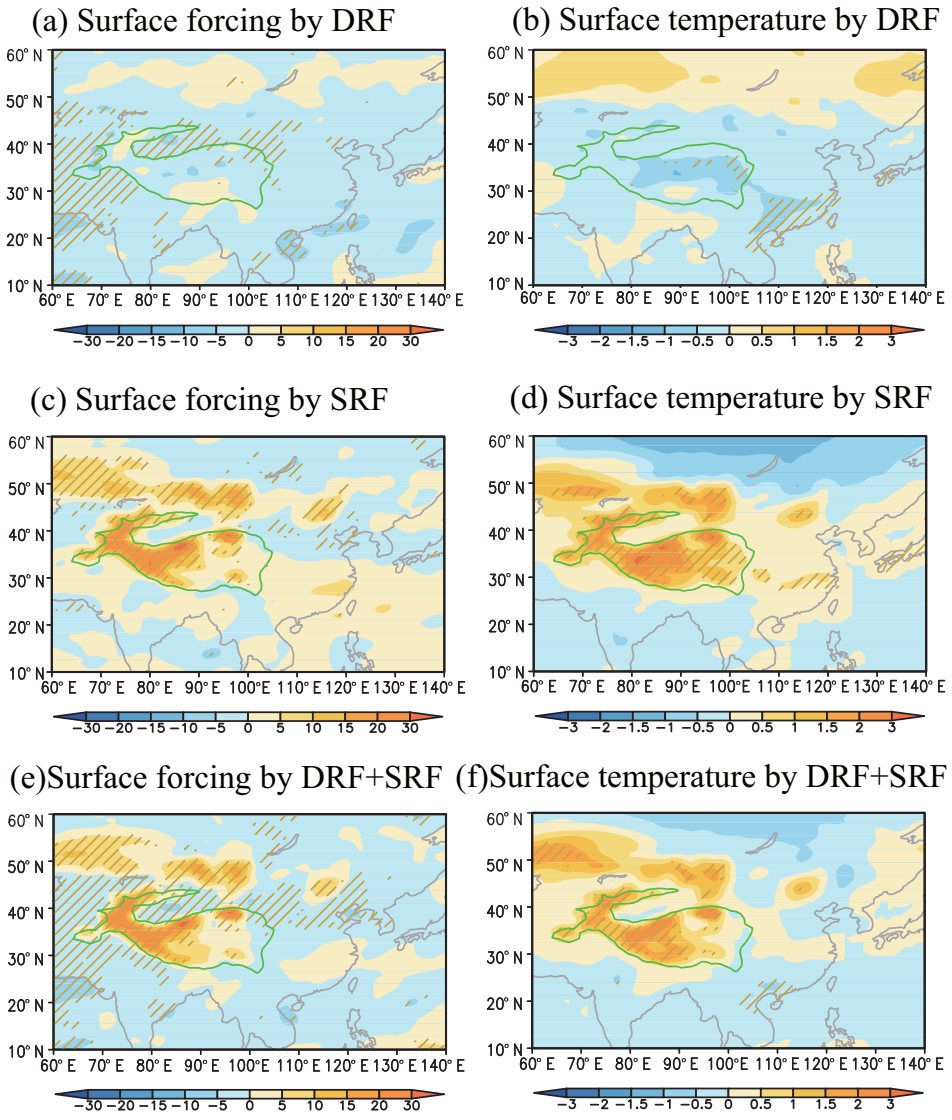

Figure 7. Spatial distribution of the changes in **(a, c, e)** the surface radiative forcing (W m^{-2}) and **(b, d, f)** the surface temperature (°C) in MAM induced by dust direct radiative forcing (DRF), dust-in-snow radiative forcing (SRF) and total radiative forcing (DRF+SRF). The slanted lines represent the grid points where the changes pass the two-tailed t test at the 5 % significance level. The green outlined area indicates the plateau above 2500 m.

Table 3. The March–April–May (MAM) averaged dust emissions (Tg per season), transport (g m^{-1} s^{-1}), dry deposition (Tg per season), and wet deposition (Tg per season) over the northern African dust source area (−20–35° E and 10–30° N) in Case1, Case2, and Case3, as well as the corresponding differences between these three experiments.

	Dust emission	Dust transport	Dry deposition	Wet deposition
Case1	276.21	2.70	177.28	16.21
Case2	292.21	2.84	187.23	16.51
Case3	268.34	2.79	168.54	14.73
DRF (Case2 − Case3)	23.87 (8.9 %)	0.05 (1.8 %)	18.69 (11.1 %)	1.78 (12.1 %)
SRF (Case1 − Case2)	−16.00 (−5.5 %)	−0.14 (−4.9 %)	−9.95 (−5.3 %)	−0.30 (1.8 %)
DRF+SRF (Case1 − Case3)	7.87 (2.93 %)	−0.09 (−3.2 %)	8.74 (5.2 %)	1.48 (10.0 %)

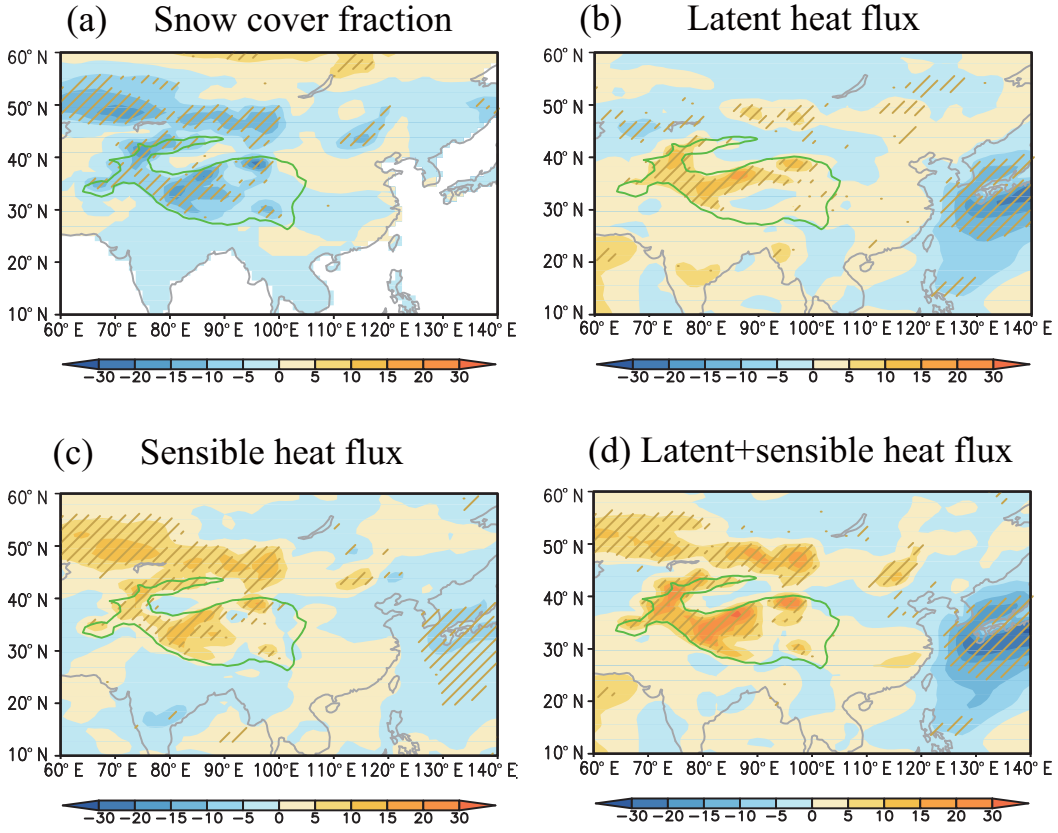

Figure 8. Spatial distribution of the changes in **(a)** the snow cover fraction (%), **(b)** the surface latent heat flux ($W\,m^{-2}$), **(c)** the surface sensible heat flux ($W\,m^{-2}$) and **(d)** the surface latent+sensible heat flux ($W\,m^{-2}$) in MAM induced by the dust-in-snow radiative forcing. Here the slanted lines in the grey shaded area represent the grid points where the changes pass the two-tailed t test at the 5 % significance level. The green outlined area indicates the plateau above 2500 m.

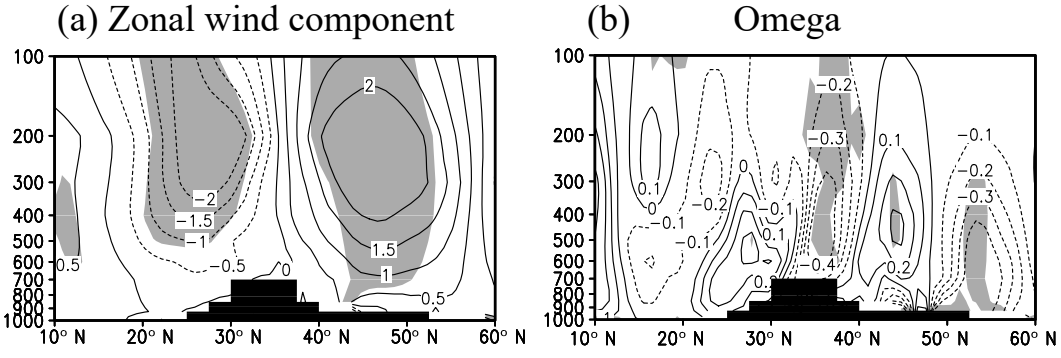

Figure 9. Changes in **(a)** the zonal wind component ($m\,s^{-1}$) and **(b)** the omega ($0.01\times Pa\,s^{-1}$) in a vertical cross section at 75–115° E in MAM induced by the dust-in-snow radiative forcing. Here the grey shaded area represents the grid points where the changes pass the two-tailed t test at the 5 % significance level. The black area indicates the plateau topography.

shows the anomalous westerly wind over the north of the TP (mainly including northwestern China) and the anomalous easterly wind forced by the SRF over the south of the TP in Fig. 9a, which are generally statistically significant over these two regions. This is because the enhanced TP thermal effect due to increasing the surface LHF and SHF induced by the SRF increases the south–north temperature gradient, resulting in a westerly wind anomaly over the north of the TP (Schiemann et al., 2009; Li and Liu, 2015). Additionally, we show the spatial distribution of the mid-level westerly winds (Fig. 10a) and the surface wind speed (Fig. 10b) over eastern Asia, indicating that the mid-level westerly winds

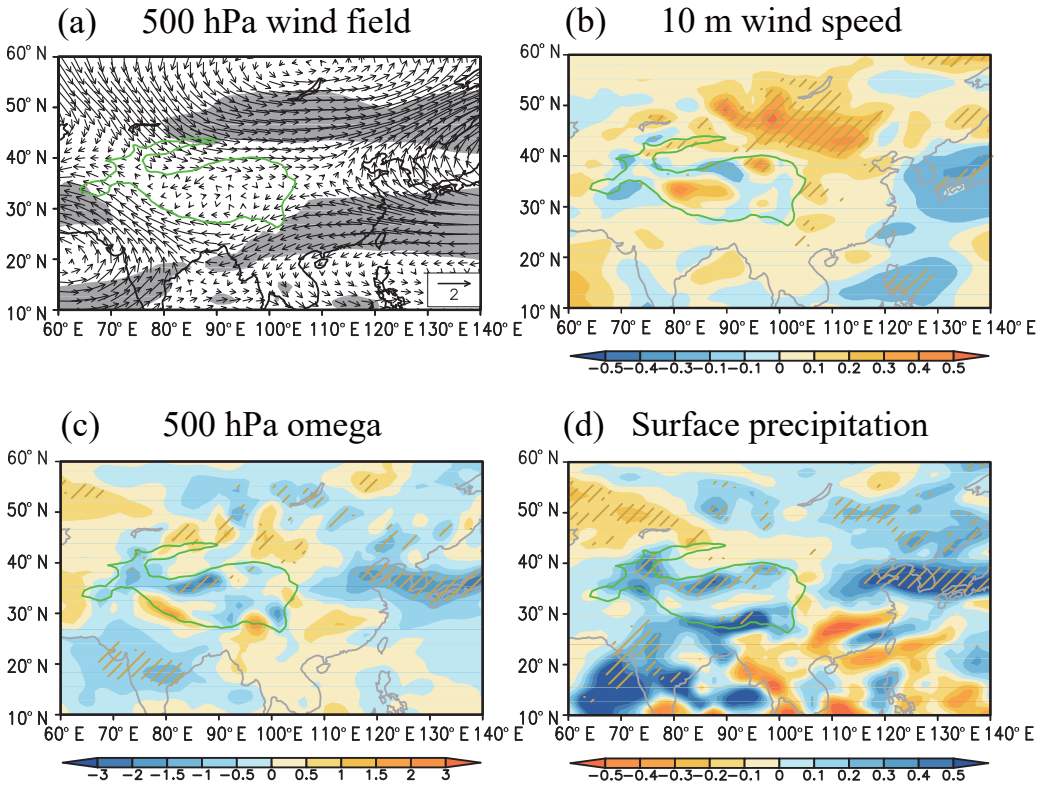

Figure 10. Spatial distribution of the changes in **(a)** the 500 hPa wind field ($m\,s^{-1}$), **(b)** the 10 m wind speed ($m\,s^{-1}$), **(c)** the 500 hPa omega ($0.01\times Pa\,s^{-1}$) and **(d)** the surface precipitation ($mm\,day^{-1}$) in MAM induced by the dust-in-snow radiative forcing. Here the slanted lines in the grey shaded area represent the grid points where the changes pass the two-tailed t test at the 5 % significance level. The green outlined area indicates the plateau above 2500 m.

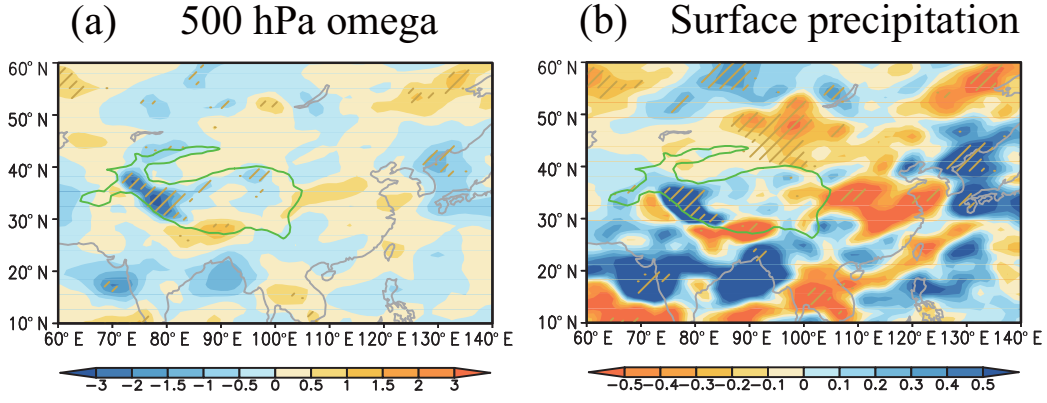

Figure 11. Spatial distribution of the changes in **(a)** the 500 hPa omega ($0.01\times Pa\,s^{-1}$) and **(b)** the surface precipitation ($mm\,day^{-1}$) in June–July–August (JJA) induced by the dust-in-snow radiative forcing. The slanted lines represent the grid points where the changes pass the two-tailed t test at the 5 % significance level. The green outlined area indicates the plateau above 2500 m.

and the surface wind speed are also significantly increased over northwestern China. The mid-level westerly winds have been recognized as one of the major factors of the long-distance dust transport process to the North Pacific Ocean, North America and beyond from eastern Asian dust sources (Wilkening et al., 2000; Guo et al., 2017), while the surface wind speed affects the dust emission rate by influencing the dust saltation process (Shao et al., 2011). Hence, the increased westerly wind affects the dust emissions and dust transport, which in turn increases the magnitude of the whole dust cycle. Additionally, the enhanced TP thermal effect induced by SRF increases the upward vertical velocity over the

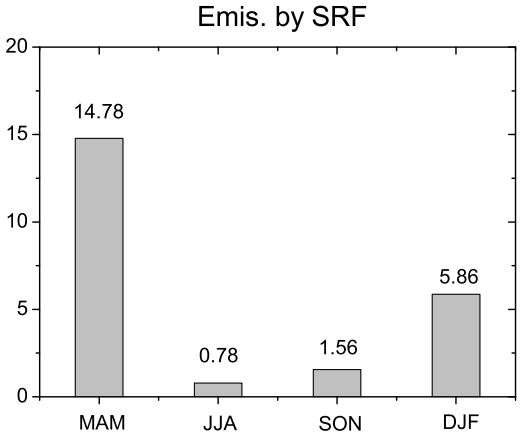

Figure 12. Seasonal changes in dust emissions (Tg per season) induced by the dust-in-snow radiative forcing (SRF) including March–April–May (MAM), June–July–August (JJA), September–October–November (SON) and December–January–February (DJF).

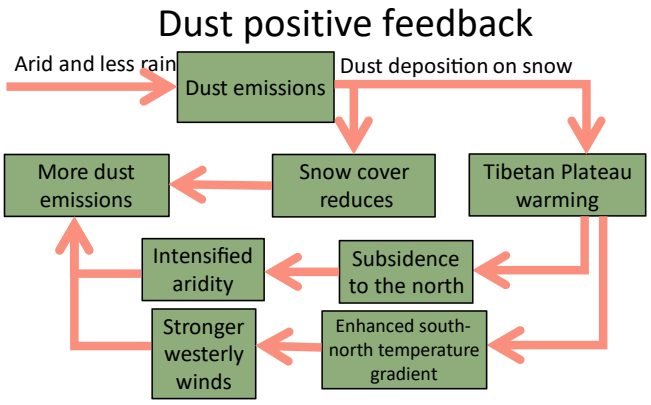

Figure 13. A schematic depiction of the feedback mechanism between dust emission and dust-in-snow radiative forcing.

TP and the downward vertical velocity (or intensifies subsidence) over northwestern China in MAM from the vertical distribution in Fig. 9b, which is also shown in Fig. 10c based on the spatial distribution. This result leads to decreased surface precipitation over northwestern China and increased surface precipitation over the TP in Fig. 10d. Note that the enhanced TP thermal effect by SRF lasts from spring to summer, which is shown in Fig. 11. It shows that the downward vertical velocity is increased in summer (Fig. 11a), resulting in significant decreased surface precipitation (Fig. 11b) over the north of the TP, whereas the upward vertical velocity and the surface precipitation are both increased over the TP. Hence, the SRF significantly decreases the surface precipitation in spring and summer and then increases the regional aridity in northwestern China, resulting in an increase of regional dust emissions. In general, the dust in snow mainly warms the TP and then increases the aridity and westerly winds through the enhanced TP thermal effects, in turn affecting the eastern Asian dust cycle.

4 Further discussion

Figure 12 shows the changes in the dust emissions by the SRF in other seasons, including JJA, SON and DJF, compared to MAM. It shows that the dust emissions are affected by the SRF in all the seasons (MAM: 14.78 Tg per season, JJA: 0.78 Tg per season, SON: 1.56 Tg per season and DJF: 5.86 Tg per season). The increase in dust emissions in MAM induced by the SRF is much larger than that in other seasons, which can account for 64 % of the annual total increase in dust emissions. This is mainly because the larger snow cover in MAM, along with the largest dust deposition, exerts significant radiative forcing, climatic feedbacks and changes in dust emissions in this season. Therefore, it is quite reasonable to focus on the dust radiative forcing and its feedbacks on the climate and dust cycle in MAM in our work.

The above results indicate the predominant causes for the SRF increasing the dust cycle over eastern Asia and is illustrated in Fig. 13. Dust aerosols are emitted from eastern Asian source regions where precipitation is limited and deposited on snow over the TP. The dust in snow over the TP reduces the surface albedo (Fig. 6b) and warms the TP (Fig. 7d), increasing the westerly winds (Fig. 9a) and the surface wind speeds (Fig. 9b) through affecting, with intensified subsidence, the south–north temperature gradient and the aridity over northwestern China (Figs. 10d and 11b). The increased aridity and stronger westerly winds can increase the dust emissions and affect the whole dust cycle (Fig. 5d, e, h, and k). Additionally, the dust in snow also accelerates snow melting, reduces snow cover (Fig. 8a), and then expands the dust source region area, resulting in an increase in dust emissions. Hence, a significant feature of SRF over the TP can create a positive feedback loop, which increases the dust emissions (as summarized in Fig. 13).

Similar to our previous study (Xie et al., 2018), we compare the changes in the eastern Asian dust cycle due to the dust radiative forcing with the northern African dust emissions. Table 3 shows that the dust emissions are significantly increased by 8.9 % due to the DRF over northern Africa, through both the strengthened large-scale circulation and the PBL mechanism (Xie et al., 2018). The changes in dust emissions caused by the SRF are much smaller than those by the DRF over northern Africa, mainly due to less snow cover and negligible SRF over this region (figures not shown). Therefore, the systematic comparative analysis reveals that the change in the dust cycle over northern Africa is dominated by DRF (Table 3), whereas it is controlled by SRF over eastern Asia due to the existence of the TP, as shown in Table 2.

5 Concluding remarks

A large amount of desert dust from eastern Asian arid and semiarid regions is deposited on snow over the Tibetan Plateau (TP). Furthermore, the dust in snow reduces the visible snow albedo by changing surface optical properties and removes the snow cover by increasing snowmelt, leading to a significant positive radiative forcing (referred to as SRF). SRF over the TP can influence the regional climate and dust cycle over eastern Asia through enhancing the TP thermal effects.

In this study, the improved CAM4-BAM model was used to investigate the SRF and its feedbacks on the climate system and the dust cycle over eastern Asia. The CAM4-BAM simulations show that SRF increases dust emissions in the spring by 14.78 Tg per season (13.7 %), thus affecting dust transport and deposition over eastern Asia. The increased effects on dust emissions by SRF are much more significant compared to the dust emissions that decreased by −8.80 Tg per season, or −7.6 % (through the PBL mechanism), induced by the dust direct radiative forcing (DRF). Simulation results show that the total effects of DRF and SRF can increase the dust emissions by 5.98 Tg per season (5.1 %). Dust in snow reduces the albedo over the TP, which warms the TP and enhances TP thermal effects and the regional dust cycle; increased sensible and latent heat fluxes from the surface result in increased aridity and westerly winds over northern China. Additionally, the dust in snow also accelerates snow melting, reduces snow cover and expands the dust source region area, resulting in an increase in dust emissions. In general, a significant feature of SRF over the TP can create a positive feedback loop to affect the dust cycle, which is summarized in Fig. 13.

It is noted that black carbon (BC) deposited on snow over the TP, mainly from southern Asia and eastern Asia (Xu et al., 2009; Wang et al., 2015), also displays a significant positive forcing over this region (Flanner et al., 2009; Qian et al., 2011). Here, we only consider the radiative forcing of the dust in snow over the TP, ignoring the radiative forcing of the BC in snow in our study. Due to the neglect of BC and dust nonlinear interactions, the dust-in-snow radiative forcing might not be accurate. Additionally, the overestimated SCF in the MAM may also artificially increase the dust-in-snow radiative forcing. The overestimated radiative forcing may amplify its feedbacks on the eastern Asian climate and dust cycle. Additionally, we focus on the eastern Asian arid and semiarid regions in order to investigate the dust cycle changes induced by SRF in this paper. Qian et al. (2011) pointed out that the radiative forcing of the absorbing aerosols can substantially influence the southern and eastern Asian monsoon climate and the regional hydrological cycle through the TP thermal effects using the CAM3.1 model.

It is noted that the atmospheric dust burden and deposition rate of dust were much higher (approximately 2 to 4 times) during the Last Glacial Maximum (LGM) compared to current climate, mainly due to increased winds speeds, the decrease in intensity of the hydrological cycle and the expansion of dust source areas (Mahowald et al., 2006; Maher et al., 2010; Albani et al., 2012). The increased dust in snow over the TP due to higher atmospheric dust loadings may show a much larger positive radiative forcing and more significantly create a positive feedback loop to affect the dust cycle in LGM. Hence, we will investigate the SRF and its feedbacks on the eastern Asian climate and the dust cycle during the LGM in the future.

Data availability. All model results are archived on the cluster system at the Institute of Earth Environment, Chinese Academy of Sciences, and available upon request. Please contact Xiaoning Xie (xnxie@ieecas.cn) for access.

Author contributions. XiaonX conducted the CAM4-BAM simulations, analyzed the results, and wrote the paper. XiaonX, XiaL, HC, XiaoxX, ZS, HW, TZ, and YL designed the study. XinL provided computational support. All authors edited the paper.

Competing interests. The authors declare that they have no conflict of interest.

Acknowledgements. This work was jointly supported by National Key Research and Development Program of China (2016YFA0601904), the Strategic Priority Research Program of Chinese Academy of Sciences (XDA20070103) and the National Natural Science Foundation of China (41690115, 41572150). Zhengguo Shi is supported by CAS "Light of West China" Program and Key Project of Air Pollution Cause and Control (DQGG0104). Yangang Liu is supported by the US Department of Energy's Atmospheric System Research (ASR) program. The data of CRU temperature are acquired from http://www.cru.uea.ac.uk/data (last access: 3 June 2013) and the data of MODIS snow cover are from https://nsidc.org/data/modis/data_summaries/T1\textbackslash#snow (last access: 21 October 2016).

Edited by: Timothy Garrett
Reviewed by: three anonymous referees

References

Albani, S., Mahowald, N. M., Delmonte, B., Maggi, V., and Winckler, G.: Comparing modeled and observed changes in mineral dust transport and deposition to Antarctica between the Last Glacial Maximum and current climates, Clim. Dynam., 38, 1731–1755, https://doi.org/10.1002/2013MS000279, 2012.

Albani, S., Mahowald, N. M., Perry, A. T., Scanza, R. A., Zender, C. S., Heavens, N. G., Maggi, V., Kok, J. F., and Otto-Bliesner, B. L.: Improved dust representation in the Commu-

nity Atmosphere Model, J. Adv. Model. Earth Sy., 6, 541–570, https://doi.org/10.1002/2013MS000279, 2014.

Ahn, H. J., Park, S. U., and Chang, L. S.: Effect of direct radiative forcing of Asian dust on the meteorological fields in east Asia during an Asian dust event period, J. Appl. Meteorol. Clim., 46, 1655–1681, 2007.

Bond, T. C., Doherty, S. J., Fahey, D. W., Forster, P. M., Berntsen, T., Deangelo, B. J., Flanner, M. G., Ghan, S., Kächer, B., Koch, D., Kinne, S., Kondo, Y., Quinn, P. K., Sarofim, M. C., Schultz, M. G., Schulz, M., Venkataraman, C., Zhang, H., Zhang, S., Bellouin, N., Guttikunda, S. K., Hopke, P. K., Jacobson, M. Z., Kaiser, J. W., Klimont, Z., Lohmann, U., Schwarz, J. P., Shindell, D., Storelvmo, T., Warren, S. G., and Zender, C. S.: Bounding the role of black carbon in the climate system: A scientific assessment, J. Geophys. Res.-Atmos., 118, 5380–5552, https://doi.org/10.1002/jgrd.50171, 2013.

Boos, W. R. and Kuang, Z.: Dominant control of the South Asian monsoon by orographic insulation versus plateau heating, Nature, 463, 218–222, 2010.

Colarco, P. R., Nowottnick, E. P., Randles, C. A., Yi, B., Yang, P., Kim, K.-M., Smith, J. A., and Bardeen, C. G.: Impact of radiatively interactive dust aerosols in the NASA GEOS-5 climate model: Sensitivity to dust particle shape and refractive index, J. Geophys. Res.-Atmos., 119, 753–786, https://doi.org/10.1002/2013JD020046, 2014.

Dang, C., Fu, Q., and Warren, S.: Effect of Snow Grain Shape on Snow Albedo, J. Atmos. Sci., 73, 3573–3583, https://doi.org/10.1175/JAS-D-15-0276.1, 2016.

Flanner, M. G., Zender, C. S., Randerson, J. T., and Rasch, P. J.: Present day climate forcing and response from black carbon in snow, J. Geophys. Res., 112, D11202, https://doi.org/10.1029/2006JD008003, 2007.

Flanner, M. G., Zender, C. S., Hess, P. G., Mahowald, N. M., Painter, T. H., Ramanathan, V., and Rasch, P. J.: Springtime warming and reduced snow cover from carbonaceous particles, Atmos. Chem. Phys., 9, 2481–2497, https://doi.org/10.5194/acp-9-2481-2009, 2009.

Flanner, M. G., Liu, X., Zhou, C., Penner, J. E., and Jiao, C.: Enhanced solar energy absorption by internally-mixed black carbon in snow grains, Atmos. Chem. Phys., 12, 4699–4721, https://doi.org/10.5194/acp-12-4699-2012, 2012.

Gu, Y., Xue, Y., De Sales, F., and Liou, K. N.: A GCM investigation of dust aerosol impact on the regional climate of North Africa and South/East Asia, Clim. Dynam., 46, 2353–2370, 2016.

Guo, J. and Yin, Y.: Mineral dust impacts on regional precipitation and summer circulation in East Asia using a regional coupled climate system model, J. Geophys. Res.-Atmos. 120, 10378–10398, https://doi.org/10.1002/2015JD023096, 2015.

Guo, J., Lou, M., Miao, Y., Wang, Y., Zeng, Z., Liu, H., He, J., Xu, H., Wang, F., Min, M., and Zhai, P.: Trans-Pacific transport of dust aerosols from East Asia: Insights gained from multiple observations and modeling, Environ. Pollut., 230, 1030–1039, 2017.

Han, Z. W., Li, J. W., Xia, X. G., and Zhang, R. J.: Investigation of direct radiative effects of aerosols in dust storm season over East Asia with an online coupled regional climate-chemistry-aerosol model, Atmos. Environ., 54, 688–699, 2012.

Hansen, J. and Nazarenko, L.: Soot climate forcing via snow and ice albedos, P. Natl. Acad. Sci. USA, 101, 423–428, 2004.

Hansen, J., Sato, M. K. I., Ruedy, R., Nazarenko, L., Lacis, A., Schmidt, G. A., Russell, G., Aleinov, I., Bauer, M., Bauer, S., and Bell, N.: Efficacy of climate forcings, J. Geophy. Res., 110, D18104, https://doi.org/10.1029/2005JD005776, 2005.

He, C., Takano, Y., and Liou, K.-N.: Close packing effects on clean and dirty snow albedo and associated climatic implications, Geophys. Res. Lett., 44, 3719–3727, https://doi.org/10.1002/2017GL072916, 2017a.

He, C., Takano, Y., Liou, K.-N., Yang, P., Li, Q., and Chen, F.: Impact of snow grain shape and black carbon-snow internal mixing on snow optical properties: Parameterizations for climate models, J. Climate, 30, 10019–10036, https://doi.org/10.1175/JCLI-D-17-0300.1, 2017b.

He, C., Liou, K.-N., Takano, Y., Yang, P., Qi, L., and Chen, F.: Impact of grain shape and multiple black carbon internal mixing on snow albedo: Parameterization and radiative effect analysis. J. Geophys. Res.-Atmos., 123, 1253–1268, https://doi.org/10.1002/2017JD027752, 2018a.

He, C., Liou, K.-N., and Takano, Y.: Resolving size distribution of black carbon internally mixed with snow: Impact on snow optical properties and albedo, Geophys. Res. Lett., 45, 2697–2705, https://doi.org/10.1002/2018GL077062, 2018b.

He, C., Flanner, M. G., Chen, F., Barlage, M., Liou, K.-N., Kang, S., Ming, J., and Qian, Y.: Black carbon-induced snow albedo reduction over the Tibetan Plateau: uncertainties from snow grain shape and aerosol–snow mixing state based on an updated SNICAR model, Atmos. Chem. Phys., 18, 11507–11527, https://doi.org/10.5194/acp-18-11507-2018, 2018c.

Heinold, B., Helmert, J., Hellmuth, O., Wolke, R., Ansmann, A., Marticorena, B., Laurent, B., and Tegen, I.: Regional modeling of Saharan dust events using LM-MUSCAT: Model description and case studies, J. Geophys. Res., 112, D11204, https://doi.org/10.1029/2006JD007443, 2007.

Heinold, B., Tegen, I., Schepanski, K., and Hellmuth, O.: Dust radiative feedback on Saharan boundary layer dynamics and dust mobilization, Geophys. Res. Lett., 35, L20817, https://doi.org/10.1029/2008GL035319, 2008.

Huang, J., Fu, Q., Zhang, W., Wang, X., Zhang, R., Ye, H., and Warren, S. G.: Dust and black carbon in seasonal snow across Northern China, B. Am. Meteorol. Soc., 92, 175–181, https://doi.org/10.1175/2010BAMS3064.1, 2011.

Huang, J., Wang, T., Wang, W., Li, Z., and Yan, H.: Climate effects of dust aerosols over East Asian arid and semiarid regions, J. Geophys. Res.-Atmos., 119, 11398–11416, https://doi.org/10.1002/2014JD021796, 2014.

Huneeus, N., Schulz, M., Balkanski, Y., Griesfeller, J., Prospero, J., Kinne, S., Bauer, S., Boucher, O., Chin, M., Dentener, F., Diehl, T., Easter, R., Fillmore, D., Ghan, S., Ginoux, P., Grini, A., Horowitz, L., Koch, D., Krol, M. C., Landing, W., Liu, X., Mahowald, N., Miller, R., Morcrette, J.-J., Myhre, G., Penner, J., Perlwitz, J., Stier, P., Takemura, T., and Zender, C. S.: Global dust model intercomparison in AeroCom phase I, Atmos. Chem. Phys., 11, 7781–7816, https://doi.org/10.5194/acp-11-7781-2011, 2011.

Hurrell, J., Hack, J., Shea, D., Caron, J., and Rosinski, J.: A new sea surface temperature and sea ice boundary data set for the Community Atmosphere Model, J. Climate, 21, 5145–5153, https://doi.org/10.1175/2008JCLI2292.1, 2008.

IPCC: Climate Change 2007: The Physical Science Basis. Contribution of Working Group I to the Fourth Assessment Report of the Intergovernmental Panel on Climate Change, edited by: Solomon, S., Qin, D., Manning, M., Chen, Z., Marquis, M., Averyt, K. B., Tignor, M., and Miller, H. L., Cambridge University Press, 996 pp., 2007.

IPCC: Climate Change 2013: The Physical Science Basis. Contribution of Working Group I to the Fifth Assessment Report of the Intergovernmental Panel on Climate Change, edited by: Stocker, T. F., Qin, D., Plattner, G.-K., Tignor, M., Allen, S. K., Boschung, J., Nauels, A., Xia, Y., Bex, V., and Midgley, P. M., Cambridge University Press, Cambridge, United Kingdom and New York, NY, USA, 1535 pp., 2013.

Kang, S. C., Xu, Y. W., You, Q. L., Flugel, W., Pepin, N., and Yao, T. D.: Review of climate and cryospheric change in the Tibetan Plateau, Environ. Res. Lett., 5, 015101, https://doi.org/10.1088/1748-9326/5/1/015101, 2010.

Kok, J. F.: A scaling theory for the size distribution of emitted dust aerosols suggests climate models underestimate the size of the global dust cycle, P. Natl. Acad. Sci. USA, 108, 1016–1021, https://doi.org/10.1073/pnas.1014798108, 2011.

Kok, J. F., Ridley, D. A., Zhou, Q., Miller, R. L., Zhao, C., Heald, C. L., Ward, D. S., Albani, S., and Haustein, K.: Smaller desert dust cooling effect estimated from analysis of dust size and abundance, Nat. Geosci., 10, 274–278, https://doi.org/10.1038/ngeo2912, 2017.

Lau, K. M., Kim, M. K., and Kim, K. M.:. Asian monsoon anomalies induced by aerosol direct forcing: the role of the Tibetan Plateau, Clim. Dynam., 26, 855–664, 2006.

Lau, K.-M., Kim, M. K., Kim, K.-M., and Lee, W. S.: Enhanced surface warming and accelerated snow melt in the Himalayas and Tibetan Plateau induced by absorbing aerosols, Environ. Res. Lett., 5, 025204 https://doi.org/10.1088/1748-9326/5/2/025204, 2010.

Lee, W.-L., Liou, K. N., He, C., Liang, H.-C., Wang, T.-C., Li, Q., Liu, Z., and Yue, Q.: Impact of absorbing aerosol deposition on snow albedo reduction over the southern Tibetan plateau based on satellite observations, Theor. Appl. Climatol., 129, 1373–1382, https://doi.org/10.1007/s00704-016-1860-4, 2017.

Lee, W. S., Bhawar, R. L., Kim, M. K., and Sang, J.: Study of aerosol effect on accelerated snow melting over the Tibetan Plateau during boreal spring, Atmos. Environ., 75, 113–122, 2013.

Li, J., Yu, R., Yuan, W., Chen, H., Sun, W., and Zhang Y.: Precipitation over East Asia simulated by NCAR CAM5 at different horizontal resolutions, J. Adv. Model. Earth Sy., 7, 774–790, https://doi.org/10.1002/2014MS000414, 2015.

Li, X., Kang, S., Zhang, G., Que, B., Tripatheea, L., Paudyal, R., Jing, Z., Zhang, Y., Yan, F., Li, G., Cui, X., Xu, R., Hu, Z., and Li, C.: Light-absorbing impurities in a southern Tibetan Plateau glacier: Variations and potential impact on snow albedo and radiative forcing, Atmos. Res., 200, 77–87, https://doi.org/10.1016/j.atmosres.2017.10.002, 2018.

Li, X. Z. and Liu, X. D.: Numerical simulation of Tibetan Plateau heating anomaly influence on westerly jet in spring, J. Earth Syst. Sci., 124, 1599–1607, 2015.

Li, Y., Wang, T., Zeng, Z., Peng, S., Lian, X., and Piao, S.: Evaluating biases in simulated land surface albedo from CMIP5 global climate models, J. Geophys. Res.-Atmos., 121, 6178–6190, https://doi.org/10.1002/2016JD024774, 2016.

Liou, K. N., Takano, Y., He, C., Yang, P., Leung, R. L., Gu, Y., and Lee, W. L.: Stochastic parameterization for light absorption by internally mixed BC/dust in snow grains for application to climate models, J. Geophys. Res.-Atmos., 119, 7616–7632, https://doi.org/10.1002/2014JD021665, 2014.

Liu, X. and Dong, B.: Influence of the Tibetan Plateau uplift on the Asian monsoon-arid environment evolution, Chinese Sci. Bull., 58, 4277–4291, https://doi.org/10.1007/s11434-013-5987-8, 2013.

Maher, B. A., Prospero, J. M., Mackie, D., Gaiero, D., Hesse, P., and Balkanski, Y.: Global connections between aeolian dust, climate and ocean biogeochemistry at the present day and at the last glacial maximum, Earth-Sci. Rev., 99, 61–97, https://doi.org/10.1016/j.earscirev.2009.12.001, 2010.

Mahowald, N. M., Muhs, D. R., Levis, S., Rasch, P. J., Yoshioka, M., Zender, C. S., and Luo C.: Change in atmospheric mineral aerosols in response to climate: Last glacial period, preindustrial, modern, and doubled carbon dioxide climates, J. Geophys. Res., 111, D10202, https://doi.org/10.1029/2005JD006653, 2006.

Mahowald, N. M., Albani, S., Kok, J. F., Engelstaedter, S., Scanza, R., Ward, D. S., and Flanner, M. G.: The size distribution of desert dust aerosols and its impact on the Earth system, Aeolian Res., 15, 53–71, https://doi.org/10.1016/j.aeolia.2013.09.002, 2014.

Meng, X., Lyu, S., Zhang, T., Zhao, L., Li, Z., Han, B., Li, S., Ma, D., Chen, H., Ao, Y., Luo, S., Shen, Y., Guo, J., and Wen, L.: Simulated cold bias being improved by using MODIS time-varying albedo in the Tibetan Plateau in WRF model, Environ. Res. Lett., 13, 044028, https://doi.org/10.1088/1748-9326/aab44a, 2018.

Miller, R. L. and Tegen, I.: Climate response to soil dust aerosols, J. Climate, 11, 3247–3267, 1998.

Ming, J., Wang, P., Zhao, S., and Chen, P.: Disturbance of light-absorbing aerosols on the albedo in a winter snowpack of Central Tibet, J. Environ. Sci.-China, 25, 1601–1607, https://doi.org/10.1016/S1001-0742(12)60220-4, 2013.

Miller, R. L., Perlwitz, J., and Tegen, I.: Feedback upon dust emission by dust radiative forcing through the planetary boundary layer, J. Geophys. Res., 109, D24209, https://doi.org/10.1029/2004JD004912, 2004.

Neale R. B., Richter, J. H., Conley, A. J., Park, S., Lauritzen, P. H., Gettelman, A., Williamson, D. L., Rasch, P. J., Vavrus, S. J., Taylor, M. A., Collins, W. D., Zhang, M., and Lin, S.-J.: Description of the NCAR Community Atmosphere Model (CAM 4.0), NCAR Tech. Note, TN–485, 212 pp., Natl. Cent. for Atmos. Res., Boulder, Colo, 2010.

Perez, C., Nickovic, S., Pejanovic, G., Baldasano, J. M., and Ozsoy, E.: Interactive dust-radiation modeling: A step to improve weather forecasts, J. Geophys. Res., 111, D16206, https://doi.org/10.1029/2005JD006717, 2006.

Perlwitz, J. P., Tegen, I., and Miller, R. L.: Interactive soil dust aerosol model in the GISS GCM: 1. Sensitivity of the soil dust cycle to radiative properties of soil dust aerosols, J. Geophys. Res., 106, 18167–18192, https://doi.org/10.1029/2000JD900668, 2001.

Qian, Y., Flanner, M. G., Leung, L. R., and Wang, W.: Sensitivity studies on the impacts of Tibetan Plateau snowpack pollution on the Asian hydrological cycle and monsoon climate, At-

mos. Chem. Phys., 11, 1929–1948, https://doi.org/10.5194/acp-11-1929-2011, 2011.

Qian, Y., Yasunari, T. J., Doherty, S. J., Flanner, M. G., Lau, W. K. M., Jing, M., Wang, H., Wang, M., Warren, S. G., and Zhang, R.: Light-absorbing Particles in Snow and Ice: Measurement and Modeling of Climatic and Hydrological impact, Adv. Atmos. Sci., 32, 64–91, https://doi.org/10.1007/s00376-014-0010-0, 2015.

Qu, B., Ming, J., Kang, S.-C., Zhang, G.-S., Li, Y.-W., Li, C.-D., Zhao, S.-Y., Ji, Z.-M., and Cao, J.-J.: The decreasing albedo of the Zhadang glacier on western Nyainqentanglha and the role of light-absorbing impurities, Atmos. Chem. Phys., 14, 11117–11128, https://doi.org/10.5194/acp-14-11117-2014, 2014.

Ramanathan, V., Crutzen, P. J., Kiehl, J. T., and Rosenfeld, D.: Aerosols, climate, and the hydrological cycle, Science, 294, 2119–2124, 2001.

Rayner, N. A., Parker, D. E., Horton, E. B., Folland, C. K., Alexander, L. V., Rowell, D. P., Kent, E. C., and Kaplan, A.: Global analyses of sea surface temperature, sea ice, and night marine air temperature since the late nineteenth century, J. Geophys. Res., 108, 4407, https://doi.org/10.1029/2002JD002670, 2003.

Schiemann, R., Lüthi, D., and Schär, C.: Seasonality and interannual variability of the westerly jet in the Tibetan Plateau region, J. Climate, 22, 2940–2957, 2009.

Schwarz, J. P., Gao, R. S., Perring, A. E., Spackman, J. R., and Fahey, D. W.: Black carbon aerosol size in snow, Sci. Rep.-UK, 3, 1356, https://doi.org/10.1038/srep01356, 2013.

Sha, Y., Shi, Z., Liu, X., and An, Z.: Distinct impacts of the Mongolian and Tibetan Plateaus on the evolution of the East Asian monsoon, J. Geophys. Res.-Atmos., 120, 4764–4782, https://doi.org/10.1002/2014JD022880, 2015.

Shao, Y., Wyrwoll, K. H., Chappell, A., Huang, J., Lin, Z., McTainsh, G. H., Mikami, M., Tanaka, T. Y., Wang, X., and Yoon, S.: Dust cycle: an emerging core theme in Earth System Science, Aeolian Res., 2, 181–204, 2011.

Shi, Z., Liu, X., Liu, Y., Sha, Y., and Xu, T.: Impact of Mongolian Plateau versus Tibetan Plateau on the westerly jet over North Pacific Ocean, Clim. Dynam., 42, 1–10, https://doi.org/10.1007/s00382-014-2217-2, 2014.

Sun, H., Pan, Z., and Liu, X.: Numerical simulation of spatial-temporal distribution of dust aerosol and its direct radiative effects on East Asian climate, J. Geophys. Res., 117, D13206, https://doi.org/10.1029/2011JD017219, 2012.

Tegen, I. and Lacis A. A.: Modeling of particle size distribution and its influence on the radiative properties of mineral dust aerosol, J. Geophys. Res., 101, 19237–19244, 1996.

Tie, X., Madronich, S., Walters, S., Edwards, D. P., Ginoux, P., Mahowald, N., Zhang, R., Lou, C., and Brasseur, G.: Assessment of the global impact of aerosols on tropospheric oxidants, J. Geophys. Res.-Atmos., 110, D03204, https://doi.org/10.1029/2004JD005359, 2005.

Wake, C. P., Mayewsi, P. A., Li, Z., Han, J., and Qin, D.: Modern eolian dust deposition in central Asia, Tellus, 46B, 220–233, 1994.

Wang, M., Xu, B., Cao, J., Tie, X., Wang, H., Zhang, R., Qian, Y., Rasch, P. J., Zhao, S., Wu, G., Zhao, H., Joswiak, D. R., Li, J., and Xie, Y.: Carbonaceous aerosols recorded in a southeastern Tibetan glacier: analysis of temporal variations and model estimates of sources and radiative forcing, Atmos. Chem. Phys., 15, 1191–1204, https://doi.org/10.5194/acp-15-1191-2015, 2015.

Wilkening, K. E., Barrie, L. A., and Engle, M.: Trans-Pacific air pollution, Science, 290, 65–67, https://doi.org/10.1126/science.290.5489.65, 2000.

Wu, G. X., Liu, Y. M., He, B., Bao, Q., Duan, A. M., and Jin, F. F.: Thermal controls on the Asian summer monsoon, Sci. Rep.-UK, 2, 1–7, 2012.

Xie, X. N., Liu, X. D., Che, H. Z., Xie, X. X., Wang, H. L., Li, J. D., Shi, Z. G., and Liu, Y.: Modeling East Asian dust and its radiative feedbacks in CAM4-BAM, J. Geophys. Res.-Atmos., 123, 1079–1096, https://doi.org/10.1002/2017JD027343, 2018.

Xu, B. Q., Cao, J., Hansen, J., Yao, T., Joswiak, D. R., Wang, N., Wu, G.,Wang, M., Zhao, H., Yang, W., Liu, X., and He, J.: Black soot and the survival of Tibetan glaciers, P. Natl. Acad. Sci. USA, 106, 22114–22118, https://doi.org/10.1073/pnas.0910444106, 2009.

Xu, Z. X., Gong, T. L., and Li, J. Y.: Decadal trend of climate in the Tibetan Plateau-regional temperature and precipitation, Hydrol. Process., 22, 3056–3065, 2008.

Yue, X., Wang, H., Wang, Z., and Fan, K.: Simulation of dust aerosol radiative feedback using the Global Transport Model of Dust: 1. Dust cycle and validation, J. Geophys. Res., 114, D10202, https://doi.org/10.1029/2008JD010995, 2009.

Zhang, D. F., Zakey, A. S., Gao, X. J., Giorgi, F., and Solmon, F.: Simulation of dust aerosol and its regional feedbacks over East Asia using a regional climate model, Atmos. Chem. Phys., 9, 1095–1110, https://doi.org/10.5194/acp-9-1095-2009, 2009.

Zhang, X. Y., Arimoto, R., and An, Z. S.: Dust emission from Chinese desert sources linked to variations in atmospheric circulation, J. Geophys. Res., 102, 28041–28047, 1997.

Zhang, Y., Kang, S., Sprenger, M., Cong, Z., Gao, T., Li, C., Tao, S., Li, X., Zhong, X., Xu, M., Meng, W., Neupane, B., Qin, X., and Sillanpää, M.: Black carbon and mineral dust in snow cover on the Tibetan Plateau, The Cryosphere, 12, 413–431, https://doi.org/10.5194/tc-12-413-2018, 2018.

Zhao, T. L., Gong, S. L., Zhang, X. Y., Blanchet, J. P., McKendry, I. G., and Zhou, Z. J.: A simulated climatology of Asian dust aerosol and its trans-Pacific transport, Part I: Mean climate and validation, J. Climate, 19, 88–103, 2006.